RSC Advances

ROYAL SOCIETY OF CHEMISTRY

www.rsc.org/advances

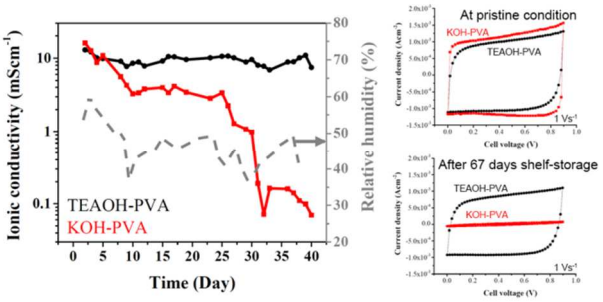

Tetraethylammonium hydroxide (TEAOH) - poly(vinyl alcohol) (PVA) electrolytes showed superior stability and shelf life to KOH-PVA electrolytes in electrochemical capacitors (ECs) .

Cite this: DOI: 10.1039/c0xx00000x

www.rsc.org/xxxxxx

ARTICLE TYPE

Alkaline quaternary ammonium hydroxides and their polymer electrolytes for electrochemical capacitors

Han Gao, Jak Li and Keryn Lian*

Received (in XXX, XXX) Xth XXXXXXXXX 20XX, Accepted Xth XXXXXXXXX 20XX

DOI: 10.1039/b000000x

Aqueous quaternary ammonium hydroxides were investigated as electrolytes for electrochemical capacitors (ECs) in both liquid and polymer-gel forms. Alkaline polymer electrolytes, composed of tetraethylammonium hydroxide (TEAOH) and poly(vinyl alcohol) (PVA) in different ratios, were developed and characterized. An optimized TEAOH-PVA electrolyte was developed and compared to KOH-PVA under controlled and ambient conditions. The stability of the polymer electrolytes and the solid ECs were characterized using cyclic voltammetry and electrochemical impedance spectroscopy. While both polymer electrolyte-based ECs demonstrated high rate capability in pristine condition, the TEAOH-based solid EC device showed a much better shelf life than the KOH-based device. This is likely due to the water retention capability of TEAOH, which promoted the amphorous phase and ion mobility, contributing to higher ionic conductivity and better environmental stability.

Introduction

Alkaline electrolytes have extensive applications in energy storage technologies from alkaline batteries, nickel-metal hydride batteries, and nickel-cadmium batteries to electrochemical capacitors (ECs or supercapacitors). Aqueous KOH electrolytes are often used in electrochemical double layer capacitors (EDLC).[1-9] Due to the involvement of hydroxide ions (OH^-), nickel oxide/hydroxide exhibits surface faradic reactions in alkaline media,[10, 11] which has been utilized in asymmetric and hybrid ECs.[12-15] For example, a commercial asymmetric cell leveraging activated carbon/nickel hydroxide in aqueous KOH has been developed by ELTON.[16]

As liquid devices exhibit leakage problems and require excess packaging, we aim to develop solid electrochemical energy storage devices. In solid devices, polymer electrolytes are key enablers to serve both as separators and as ionic conductors.[17] Most aqueous-based polymer electrolytes are fabricated by blending polymer host materials with ionic conductors, water, and plasticizers.[18] For alkaline-based polymer electrolytes, the conduction of OH^- is highly dependent on two factors: (a) the presence of water in the "swollen" polymer matrix such that both vehicle and hopping mechanisms contribute to ion conduction;[19] and (b) the amorphous phase of the polymer electrolyte where segmental motions of the polymer chains enhance ion mobility.

Poly(vinyl alcohol) (PVA) exhibits excellent properties as a polymer host due to its high hydrophilicity and good film forming capability. Extensive studies have been performed on KOH-PVA systems as OH^- conducing polymer electrolytes,[20-23] but less attention has been paid to the stability of KOH-PVA over time, especially in an ambient environment. Dehydration of KOH-PVA has a detrimental impact on its ionic conductivity as the removal of water limits ion conduction in the polymer electrolyte. In addition, the crystallization of KOH during film dehydration affects film integrity and continuity, resulting in severely decreased conductivity.

Alternatively, quaternary ammonium hydroxides, for example, tetramethylammonium hydroxide (TEAOH), can be used as OH^- conductors for alkaline polymer electrolytes. The cations have a general structure of NR_4^+ where R can be an alkyl group or an aryl group. These organic compounds are miscible with water at room temperature, which allows for easy preparation of the electrolyte precursor solutions. In addition, the crystallization limit of quaternary ammonium hydroxides is much higher than for KOH in salt-water binary systems.[24] Table 1 lists relevant properties of tetramethylammonium (TMA^+), tetraethyl-ammonium (TEA^+), tetrabutylammonium (TBA^+), and K^+ in aqueous solutions. The quaternary ammonium ions showed lower diffusivity than K^+ at room temperature due to their larger ion size. Among the three quaternary ammonium ions, TBA^+ showed the largest ionic radius and the lowest diffusivity. Also shown in Table 1 are the hydrated ionic radii of these cations, which decrease in the order $TBA^+ > TEA^+ > TMA^+ > K^+$, inverse proportional to their mobility. However, the slight increase in the size of hydrated TMA^+ or TEA^+ ions may not significantly impact conductivity and double layer capacitance as compared to K^+ ions, especially when integrated in polymer electrolytes.

Table 1 Room temperature diffusivity, stoke ionic radius, and hydrated ionic radius of TMA^+, TEA^+, TBA^+, and K^+ ions in aqueous solutions[25, 26]

	TMA^+	TEA^+	TBA^+	K^+
Diffusivity ($\times 10^{-5}$ cms^{-1})[a]	1.20	0.87	0.62-0.48	1.96
Stoke ionic radius (Å)	2.05	2.82	4.72	1.25
Hydrated ionic radius (Å)	3.67	4.0	4.94	3.31

[a] At infinite dilution.

Polymer electrolytes leveraging quaternary ammonium hydroxides have been used in fuel cells. For example, grafting of quaternary ammonium cationic groups onto an aromatic ring is a common practice to produce anion exchange membranes for alkaline full cells and has shown high performance and stability.[27] Considering their advantages such as miscibility with water and a high crystallization limit for enhanced stability, this study aimed to introduce quaternary ammonium hydroxides into solid ECs.

Our objective was to develop novel alkaline polymer electrolytes that can perform equal or better than KOH-based polymer electrolytes for ECs. In this paper, we first compared several aqueous quaternary ammonium hydroxides, tetramethylammonium hydroxide (TMAOH), tetraethylammonium hydroxide (TEAOH), and tetrabutylammonium hydroxide (TBAOH), against KOH in terms of their ionic conductivity and capacitance in a metallic double layer EC platform. We selected TEAOH as the most suitable ionic conductor to integrate into a polymer electrolyte. Subsequently, solid ECs utilizing metallic or graphite electrodes with either a TEAOH-based polymer electrolyte or a KOH-based polymer electrolyte were assembled. The electrochemical behavior of these solid ECs was investigated and compared to evaluate the feasibility and stability of the polymer electrolytes for applications in ECs.

Experimental

Electrolyte preparation

Aqueous electrolytes based on KOH and three quaternary ammonium hydroxides (TMAOH, TEAOH, and TBAOH) were prepared in three concentrations: 0.1 M, 0.5 M, and 1 M. To produce polymer electrolyte films, aqueous precursor solutions were mixed from a combination of PVA (MW=145,000) and hydroxide solutions in different weight ratios (or molar ratios) as shown in Table 2. An optimized TEAOH-PVA electrolyte was selected and compared to KOH-PVA prepared with an equal salt to polymer molar ratio.

Table 2 Summary of different TEAOH : PVA ratios for polymer electrolyte preparation

Sample	TEAOH : PVA weight ratio[a]	TEAOH : PVA molar ratio[a]
TEAOH-PVA(52-48)	52 : 48	1055 : 1
TEAOH-PVA(68-32)	68 : 32	2110 : 1
TEAOH-PVA(76-24)	76 : 24	3165 : 1
TEAOH-PVA(81-19)	81 : 19	4220 : 1
TEAOH-PVA(87-13)	87 : 13	6330 : 1

[a] Calculated based on ignoring the water content in the film.

Material Characterizations

Infrared (IR) spectra were recorded at room temperature on a Thermo Scientific Nicolet iS5 FT-IR spectrometer with iD1 transmission module. A liquid electrolyte or a polymer electrolyte solution was added on the central portion of an IR transparent Si window. The water was allowed to evaporate under ambient conditions for 30 minutes to form a thin film with uniform thickness. A removable mask was placed on the Si window to control the area and thickness of the resulting film. All samples for IR spectroscopy were prepared and characterized on the same day and under the same conditions (25 °C, 20% RH) to avoid influence of temperature and relative humidity.

X-ray diffraction (XRD) measurements were carried out using a Philips XRD system, including a PW 1830 HT generator, a PW 1050 goniometer, and PW3710 control electronics. The samples were analyzed with a Cu-Kα source operating at 40 kV/40 mA. The diffraction patterns were recorded from 5° to 50° 2θ with a step scan of 0.02° 2θ. All XRD samples were prepared at 25 °C, 40% RH.

Thermogravimetric analyses (TGA) were carried out in a TGA Q500 in an Argon environment from 30 to 120 °C. All TGA film samples were prepared and equilibrated at 25 °C, 40% RH.

An HI 9811 pH/EC/TDS meter (HANNA instruments) was used to measure the pH of the aqueous electrolytes. A pH buffer solution (HI 7010 at pH 10.01) was used for calibration.

Electrochemical characterizations

For aqueous electrolyte characterization, two smooth nickel foils with 3 mm spacing were used to construct a liquid test vehicle. The geometric area of the electrode was 1 cm^2, all other exposed areas were covered with surface protection tape (American Biltrite) and chemically resistant epoxy (Buehler).

To determine the performance of the polymer electrolytes as well as of the resulting solid ECs, two types of electrodes were employed in the cell assemblies: (a) Ni as metallic electrodes and (b) graphite as EDLC electrodes. An aqueous based graphite conductive ink (Alfa Aesar) was coated on Ni foils and dried in air to form graphite electrodes. The loading of graphite was 5 $mgcm^{-2}$. The geometric area of all electrodes for solid cells was 1 cm^2. To construct solid ECs, the polymer electrolyte precursor solution was directly cast on the electrodes, forming a polymer electrolyte film with a thickness between 80 μm to 100 μm. Solid ECs were assembled by sandwiching the electrolyte film between two electrodes under pressure with tape packaging.

Both liquid and solid ECs were characterized by cyclic voltammetry (CV) and electrochemical impedance spectroscopy (EIS) using a CHI 760C bipotentiostat. The ionic conductivity of all electrolytes was calculated based on the equivalent series resistance (ESR) of the ECs and their geometric surface area as well as the spacing of the electrodes (or thickness of the polymer electrolyte). Areal capacitance of the cells was calculated using charge divided by voltage window and geometric surface area. All tests were conducted under ambient conditions.

Results and discussion

Aqueous electrolyte characterization

TMAOH, TEAOH, and TBAOH were first studied and compared with KOH in their respective aqueous solutions. To characterize the degree of ionic dissociation of these aqueous electrolytes, the pH of the solutions in different concentrations was measured and is shown in Fig.1. For all aqueous electrolytes, pH increased with concentration as expected. However, all three quaternary ammonium hydroxides showed a higher pH than KOH, indicating a higher degree of ionic dissociation. Among the three quaternary ammonium hydroxides, the TMAOH and TEAOH solutions exhibited a higher basicity than TBAOH. The ionic conductivity of the quaternary ammonium hydroxides and KOH was measured as a function of concentration and is shown in Fig. 1b: Conductivity increased with concentration for all electrolytes. As

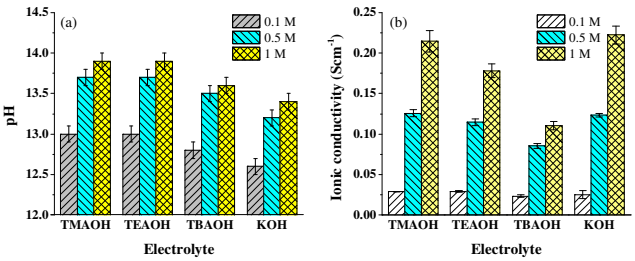

Fig. 1 Comparison of (a) pH and (b) ionic conductivity of aqueous TMAOH, TEAOH, TBAOH, and KOH electrolytes in different concentrations at 298 K

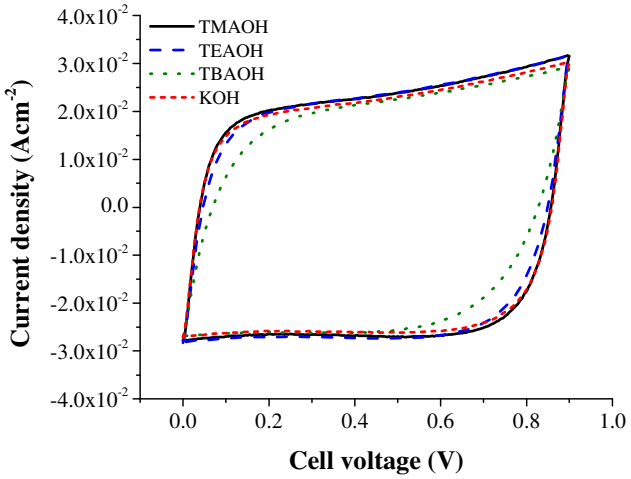

Fig. 2 CV comparison of 1 M liquid aqueous TMAOH, TEAOH, TBAOH, and KOH metallic cells at a 5000 Vs-1 scan rate

a baseline, the ionic conductivity of 1 M was 0.22 Scm^{-1}, which agrees with the value reported by Gilliam under similar conditions.[28] Although the relatively large cations of the TMAOH and TEAOH solutions somewhat limited cation mobility (Table 1), both showed conductivity comparable to the KOH solution due to their stronger ionic dissociation. On the other hand, TBAOH exhibited the lowest ionic conductivity among the four solutions due to a large size and a lower degree of ionic dissociation (comparable to KOH). Fig. 2 shows the overlaid CVs of all four liquid cells in 1 M solutions at an ultra-high scan rate of 5000 Vs^{-1}. At this high scan rate, the cell response is dominated by the kinetics of charge separation or ion movement. Both TMAOH and TEAOH liquid cells had a capacitance comparable to that of the liquid KOH cell. TBAOH had the lowest capacitance and the highest resistance at this scan rate due to its low ionic conductivity and ionic dissociation. While both TMAOH and TEAOH are good alternative electrolytes to KOH for ECs in terms of ionic conductivity and capacitance, TEAOH was selected as the basis for the polymer electrolytes due to its more environmentally benign nature.

FTIR characterization of the polymer electrolytes

TEAOH-PVA polymer electrolytes were prepared in 5 different ratios (Table 2). FTIR analysis was performed on TEAOH-PVA polymer electrolytes to obtain structural, compositional, and bonding information. To better understand the interactions

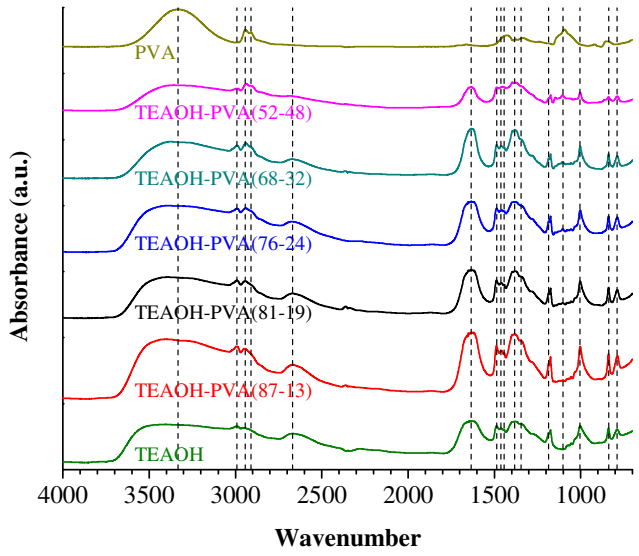

Fig.3 IR spectra of TEAOH-PVA polymer electrolytes pure PVA, and pure TEAOH

between TEAOH and PVA in the polymer electrolytes, a pure TEAOH solution and a pure PVA film were characterized as baselines. Fig. 3 presents the IR spectra of pure PVA, TEAOH, and TEAOH-PVA polymer electrolytes. The bands and related bonding information are summarized in Table 3.

In the wavenumber region from 4000 to 2000 cm^{-1}, common bands of OH stretching, CH_2 stretching, and CH stretching are observed for all samples. With the addition and increase of TEAOH in PVA, a new band representing CH_3 stretching can be identified. Both CH_2 stretching and CH stretching bands showed a decrease in their intensity, resulting from the reduction in PVA content in the polymer electrolytes. In addition, OH bending peaks at 1634 cm^{-1} were observed for all the polymer electrolytes as well as the TEAOH solution due to the presence of water molecules. In contrast, the dry PVA film did not show the OH bending of water molecules.

At lower wavenumbers from 2000 to 700 cm^{-1}, some of the characteristic TEAOH peaks could be identified in the polymer electrolytes. These include CH_3 bending at 1488 and 1382 cm^{-1}, C-C-N bands at 1186 and 1003 cm^{-1}, CH_3 rocking at 838 cm^{-1}, and NC_4 stretching at 788 cm^{-1}. These peaks showed an increase in intensity with the increase of TEAOH content. Conversely, the characteristic peaks of PVA, such as CH_2 bending at 1426 cm^{-1}, CH_2 twisting at 1333 cm^{-1}, and CO stretching at 1093 cm^{-1}, decreased and even vanished with higher TEAOH content. Comparing the FTIR spectrum of TEAOH-PVA with the spectra of its individual components (Fig. 3 and Table 3), all bands for TEAOH-PVA can be related to its individual components; no additional bands are observed. This indicates that the TEAOH structure was retained in the polymer electrolytes over the range of polymer ratios in the various TEAOH compositions. These observations confirmed the successful blending between TEAOH and PVA in our polymer electrolytes.

To achieve high ionic conductivity in the polymer electrolytes, the presence of water plays an important role as ion conduction media. To understand the interaction between TEAOH or PVA and water, we focus on the OH stretching band of the polymer electrolytes. With the addition of TEAOH into PVA, as a result

Table 3 FTIR band positions and associated bonding information for TEAOH-PVA, pure TEAOH, and pure PVA

PVA[a]	Wavenumber TEAOH-PVA(52-48)	TEAOH-PVA(68-32)	TEAOH-PVA(76-24)	TEAOH-PVA(81-19)	TEAOH-PVA(87-13)	TEAOH	Band Assignment
3332	3354	3376	3382	3394	3401	3404	OH stretching
	2991	2992	2992	2992	2992	2992	CH_3 stretching
2943	2937	2939	2940	2943	2946	2953	CH_2 stretching
2910	2907						CH stretching
	2687	2672	2673	2670	2669	2668	N/A
	1634	1634	1633	1634	1633	1633	OH bending of H_2O
	1486	1487	1487	1488	1488	1488	CH_3 asymmetric bending
	1462	1462	1462	1462	1462	1462	CH_2 bending
1426	1443	1443	1443	1443	1443	1443	CH_2 symmetric bending
	1373	1381	1381	1382	1382	1382	CH_3 bending
1333	1346	1346	1346	1346	1346	1345	CH_2 twisting
	1185	1185	1185	1186	1186	1186	C-C-N
1093	1105	1104	1104	1104	1104	1104	CO stretching
	1003	1003	1003	1003	1003	1003	C-C-N
	839	839	839	839	839	838	CH_3 rocking
	788	788	788	788	788	788	NC_4 stretching

[a] Free-standing film

of strong hydrogen bond interactions in the TEAOH-PVA system, a broadening of the OH stretching bands was observed for all electrolytes. In addition, a shift of OH stretching towards higher frequencies with increasing TEAOH content was observed in TAOH-PVA electrolyte films (from 3354 to 3401 cm^{-1}, see Table 3). This shift was due to a decrease in hydrogen bonding that resulted from the dehydration of the films. Although the increased TEAOH content enhances the ionic conductivity of TEAOH-PVA polymer electrolytes, it may also cause faster film dehydration and degradation. This will eventually limit ion mobility and reduce environmental stability.

Ionic conductivity of the polymer electrolytes

In order to investigate the influence of TEAOH content on the conductivity and environmental stability of the polymer electrolytes, the conductivity of TEAOH-PVA at different ratios was measured over a period of 2 months in an ambient environment (Fig. 4). The general trend shows the average conductivity increasing with increasing TEAOH content. TEAOH-PVA(87-13) showed the highest average conductivity of 0.013 Scm^{-1}, while TEAOH-PVA(52-48) showed the lowest average conductivity of 0.001 Scm^{-1}. However, the films with high PVA content showed the best environmental stability with minimal variation in conductivity over time. This was in a good agreement with the FTIR results which showed that increased PVA content both promoted the hydrogen bond interaction between TEAOH, PVA, and water molecules as well as lowered the kinetics of dehydration. Although TEAOH-PVA(87-13) was more conductive than TEAOH-PVA(81-19), it exhibited greater fluctuation in conductivity. Therefore, TEAOH-PVA(81-19) was selected as the optimized polymer electrolyte for further characterization.

To compare the performance of the TEAOH-PVA(81-19) electrolyte with a KOH-PVA system, KOH-PVA films were prepared with the same molar ratio of 4220:1 (Table 2). Fig. 5a

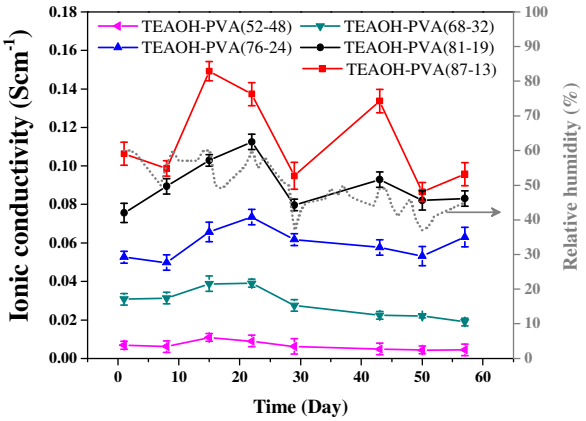

Fig. 4 Ionic conductivity tracking of TEAOH-PVA polymer electrolytes over time under ambient conditions

depicts the ionic conductivity of TEAOH-PVA and KOH-PVA as a function of time under ambient conditions. Although the initial conductivity of KOH-PVA was higher than that of TEAOH-PVA, it showed a significant reduction over time; eventually its conductivity dropped to two orders of magnitude below that of TEAOH-PVA. TEAOH-PVA, in contrast, showed stable performance with an average conductivity of 0.01 Scm^{-1} throughout the 2-month test period.

The loss of conductivity in KOH-PVA may be due to film dehydration, causing crystallization of KOH in the PVA matrix. This leads to a high activation energy barrier for ion transportation. To compare the crystallization of KOH and TEAOH in PVA, Fig. 5b shows photographs of a TEAOH-PVA film and a KOH-PVA film cast on a glass slide and stored in an ambient environment for 3 days. The TEAOH-PVA film retained its gel and translucent form while the KOH-PVA film exhibited a large extent of salt crystallization, significantly reducing film flexibility and continuity.

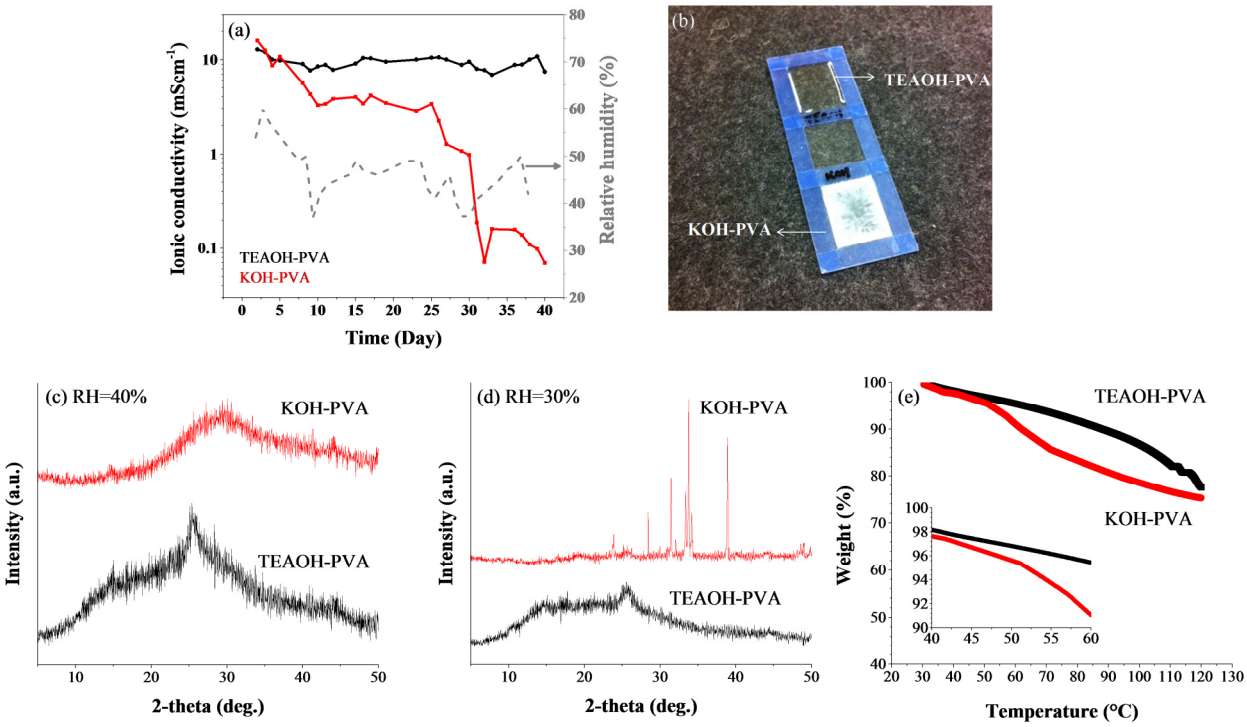

Fig. 5 (a) Ionic conductivity of polymer electrolyte TEAOH-PVA (●) and KOH-PVA (■), demonstrating their stability over time; (b) a photograph of a TEAOH-PVA film and a KOH-PVA film cast on a glass slide; and powder XRD patterns of TEAOH-PVA and KOH-PVA films (c) in pristine condition of 40% RH and (d) after a 3 days storage under ambient conditions (RH=30%); (e) TGA graphs of TEAOH-PVA and KOH-PVA films both equilibrated at 40% RH. The inset is the enlarged view from 40 to 60°C.

XRD and TGA characterizations of the polymer electrolytes

The ionic conductivity of a polymer electrolyte depends on two factors: a) the presence of water (for ion-hopping between coordinate sites and vehicle mechanism) and b) local structural relaxation and segmental motions of the polymer host. We examined the level of film hydration/dehydration as well as the crystallinity of TEAOH-PVA and KOH-PVA by XRD (Fig. 5c and 5d).

In pristine condition (RH=40%), both TEAOH-PVA and KOH-PVA films showed highly amorphous structure (Fig. 5c). The broad peak at 25° 2θ in TEAOH-PVA corresponds to TEAOH•$5H_2O$[29] while the broad peak at 30° 2θ in KOH-PVA confirms the presence of KOH.[30] The same polymer electrolyte films were analyzed after 3 days of shelf storage under ambient conditions (RH=30%); the resulting XRD patterns are shown in Fig. 5d.

Both TEAOH-PVA and KOH-PVA showed a certain extent of dehydration. However, TEAOH-PVA showed a much slower dehydration than its KOH counterpart. The small peak at 15° 2θ in TEAOH-PVA indicates the presence of TEAOH•$4H_2O$[31], due to the dehydration of TEAOH from its pentahydrate form to its tetrahydrate form. KOH, on the other hand, rapidly crystallized in the polymer matrix. Crystallization of KOH in an aqueous solution begins around 54 wt. % (i.e., 24 mol %) at room temperature[32] to form KOH•$2H_2O$, while TEAOH in an aqueous solution crystallizes at a concentration twice as high as that of KOH (50 mol %) at room temperature[24]. Therefore, the higher tolerance for TEAOH crystallization has resulted in a better retention of the amorphous phase in TEAOH-PVA. In addition, even with the crystallization of TEAOH in the electrolyte, TEAOH-PVA has more water molecules incorporated in the crystal structure and thus shows a higher degree of hydration than the KOH-PVA electrolyte.

The water retention capability of TEAOH-PVA and KOH-PVA films equilibrated at 40% RH was further examined through TGA (Fig. 5e). Both samples showed a continuous decrease in weight due to loss of water. TEAOH-PVA exhibited a smaller reduction than the KOH-PVA electrolyte over the temperature range. This suggests that water molecules are more difficult to release from the TEAOH-PVA electrolyte. Further, while TEAOH-PVA film showed some fluctuation in weight loss and a sharp decay beyond 110°C, KOH-PVA exhibited a decreased decline in weight loss at high temperatures. This can be explained by the difference of the phases between TEAOH and KOH: TEAOH is a liquid with a boiling point around 97°C while KOH, especially after dehydration, is solid. Overall, TEAOH-PVA dehydrated slower and tolerated changes in the environment better over the application temperature range, which makes it more viable as electrolyte for energy storage.

Metallic cell performance

CVs of both TEAOH-PVA and KOH-PVA solid metallic cells in pristine condition are shown in Fig. 6a. Both cells showed a comparable double-layer capacitance of ca. 8 μFcm^{-2} at 5000 Vs^{-1} with a rectangular CV profile, indicating good capacitive behavior. The capacitance is similar to liquid devices (Fig. 2), suggesting both polymer electrolytes can transfer ions at very high speeds and retain good ionic accessibility at the electrode surface. Fig. 6b shows the CVs of the solid cells at the same

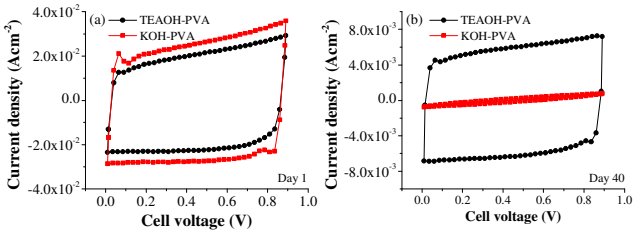

Fig. 6 CVs of a solid metallic/TEAOH-PVA EC (●), and a solid metallic/KOH-PVA EC (■) at (a) day 1, and (b) day 40 (sweep rate=5000 Vs^{-1})

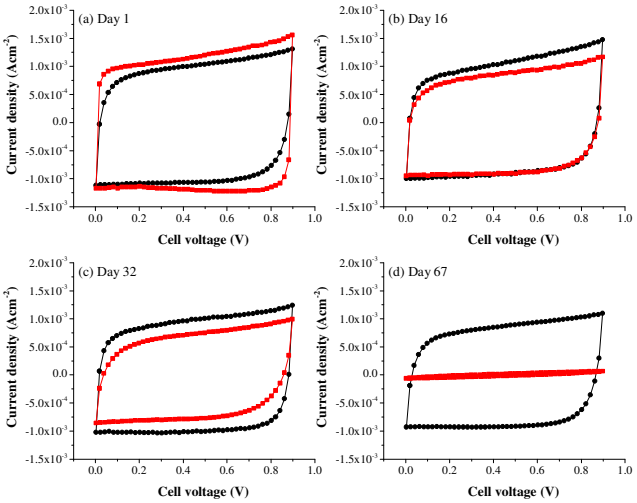

Fig. 7 CVs of a solid graphite/TEAOH-PVA EC (●) and a solid graphite/KOH-PVA EC (■) at (a) day 1, (b) day 16, (c) day 32, and (b) day 67 (sweep rate=1 Vs^{-1})

sweep rate, but after 40 days of shelf storage. The solid TEAOH-PVA cell retained ca. 50% of its capacitance and a rectangular CV profile. In contrast, the KOH-PVA cell suffered from a sharp decrease in capacitance and an increase in cell ESR. The destruction of the electrode/electrolyte interface and the severe reduction in ionic conductivity significantly limited the performance of the solid KOH-PVA cell.

Graphite cell performance

Since the intended application of the polymer electrolytes is for thin film ECs, solid symmetric EDLC devices were constructed using graphite electrodes and the polymer electrolytes. Fig. 7 overlays the CVs of a graphite/TEAOH-PVA EC and a graphite/KOH-PVA EC after various durations of shelf-storage (all at 1 Vs^{-1}). In pristine condition (Fig. 7a), the graphite/KOH-PVA EC showed a higher capacitance compared to the graphite/TEAOH-PVA EC similar to the trend from solid metallic ECs (Fig. 6a). The lower cell ESR also confirmed the higher ionic conductivity of the as-prepared KOH-PVA film (Fig. 5a). Fig. 7a-7d shows the CVs of these solid ECs at the same sweep rate, but after 16, 32, and 67 days of shelf storage, respectively. The graphite/KOH-PVA EC showed a continuous decrease in capacitance. As shown in Fig. 7d, the graphite/KOH-PVA EC reached the end of its service life after two months of shelf storage. In contrast, the solid graphite/TEAOH-PVA EC retained its capacitance and capacitive behavior over the same

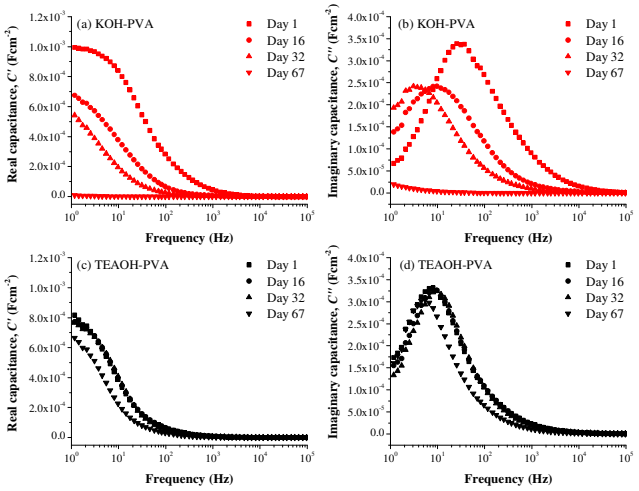

Fig. 8 Electrochemical impedance spectroscopy profiles showing the real part and the imaginary part of capacitance vs. frequency for (a, b) a solid graphite/KOH-PVA EC and (c, d) a solid graphite/TEAOH-PVA EC at day 1, day 16, day 32, and 67

period. Both graphite/TEAOH-PVA EC and graphite/KOH-PVA EC showed better stability compared to their metallic cell counterparts (Fig. 6). This may be attributed to less destruction at the electrode/electrolyte interface caused by dehydration of carbon electrodes as compared to smooth metallic electrodes, resulting in an increase in the stability of both graphite cells.

Further investigation of the solid graphite ECs was performed using EIS. We separated the real part of the capacitance (C') from its imaginary part (C'')[33] and plotted them as a function of frequency (Fig. 8a-8d). The real capacitance (C') represents the accessible capacitance while the maximum of the imaginary capacitance (C'') vs. frequency curve represents a time constant. The latter is used as a ''factor of merit'' to compare the rate capability of ECs. Table 4 summarizes the capacitance and time constants of the two devices. The areal capacitances of the solid graphite/TEAOH-PVA device and the solid graphite/KOH-PVA device reached 0.8 mFcm^{-2} and 1 mFcm^{-2}, respectively, at day 1, agreeing with the CV results (Fig. 7a). Due to the higher ionic conductivity of KOH-PVA in pristine condition, the graphite/KOH-PVA EC exhibited a faster device response even with a higher cell capacitance, indicated by a small time constant of 39 ms. The impedance of both devices was again measured after 16, 32, and 67 days of shelf storage. As shown in Fig. 8c and 8d, the solid graphite/TEAOH-PVA EC retained its C' and C'' values over the testing period (Table 4). The solid graphite/KOH-PVA EC exhibited a loss of capacitance over all frequencies and the time constant peak of its imaginary capacitance (C'') shifted to much lower frequencies as a result of considerably increased cell ESR.

Both Fig. 7 and 8 provide strong evidence that the TEAOH-PVA polymer electrolyte is able to transport ions under ambient conditions and has good environmental stability. Although the graphite/KOH-PVA EC initially had excellent high rate performance, the graphite/TEAOH-PVA EC demonstrated much better shelf life, rendering it a better candidate for low to room temperature solid electrochemical devices. Further optimization of the TEAOH-PVA electrolyte system is under way to improve its conductivity and environmental stability under extreme

Table 4 Variations of capacitance and time constants of a graphite/TEAOH-PVA EC and a graphite/KOH-PVA EC, obtained from electrochemical impedance spectroscopy over time

Graphite cell	**Capacitance ($mFcm^{-2}$)[a]**			
	Day 1	Day 16	Day 32	Day 67
TEAOH-PVA	0.817	0.774	0.767	0.685
KOH-PVA	0.994	0.675	0.542	0.008
Graphite cell	**Time constant (ms)**			
	Day 1	Day 16	Day 32	Day 67
TEAOH-PVA	123.9	123.9	102.4	182.3
KOH-PVA	38.9	102.4	323.6	N/A

[a] At 1 Hz.

conditions. In addition, the ion conduction mechanisms in TEAOH-PVA as well as its interactions with pseudocapacitive electrodes (i.e. with faradaic reactions) are under investigation.

Conclusions

In this comparative study of quaternary ammonium hydroxides and KOH, both TMAOH and TEAOH solutions proved to be suitable alternative aqueous electrolytes to KOH for EC applications, in terms of ionic conductivity and capacitance in liquid cells. To develop optimal polymer electrolytes using the quaternary ammonium hydroxides, molecular interactions and ionic conductivity of polymer electrolytes composed of TEAOH and PVA in different ratios were characterized. An optimized TEAOH-PVA electrolyte was developed, balancing ionic conductivity and environmental stability. To demonstrate the performance of this polymer electrolyte, solid EC devices based on TEAOH-PVA and KOH-PVA were assembled using metallic and graphite electrodes. Both TEAOH-PVA and KOH-PVA performed well in pristine condition, as demonstrated by their respective ECs. However, the sensitivity of KOH-PVA to dehydration and the crystallization of KOH limited its performance over time in an ambient environment, resulting in short shelf-life. In contrast, high ionic conductivity, good film forming capability, and high environmental stability make TEAOH-PVA an attractive alkaline polymer electrolyte system for electrochemical devices.

Acknowledgments

We appreciate the financial support of NSERC Canada and Ontario Research Fund. H. Gao would like to acknowledge an NSERC Alexander Graham Bell Canada Graduate Scholarship.

Notes

Department of Materials Science and Engineering, University of Toronto, 184 College Street, Suite 140, Toronto, Ontario M5S 3E4, Canada.
E-mail: keryn.lian@utoronto.ca

References

1. J. R. Miller, R. Outlaw and B. Holloway, *Science*, 2010, **329**, 1637-1639.
2. K. Sheng, Y. Sun, C. Li, W. Yuan and G. Shi, *Sci. Rep.*, 2012, **2**.
3. W. Xing, S. Z. Qiao, R. G. Ding, F. Li, G. Q. Lu, Z. F. Yan and H. M. Cheng, *Carbon*, 2006, **44**, 216-224.
4. C.-W. Huang, C.-H. Hsu, P.-L. Kuo, C.-T. Hsieh and H. Teng, *Carbon*, 2011, **49**, 895-903.
5. E. Frackowiak, *PCCP*, 2007, **9**, 1774-1785.
6. M. D. Stoller, S. Park, Y. Zhu, J. An and R. S. Ruoff, *Nano Lett.*, 2008, **8**, 3498-3502.
7. V. L. Pushparaj, M. M. Shaijumon, A. Kumar, S. Murugesan, L. Ci, R. Vajtai, R. J. Linhardt, O. Nalamasu and P. M. Ajayan, *Proceedings of the National Academy of Sciences*, 2007, **104**, 13574-13577.
8. J. Yan, J. Liu, Z. Fan, T. Wei and L. Zhang, *Carbon*, 2012, **50**, 2179-2188.
9. E. Raymundo-Piñero, K. Kierzek, J. Machnikowski and F. Béguin, *Carbon*, 2006, **44**, 2498-2507.
10. K.-W. Nam and K.-B. Kim, *J. Electrochem. Soc.*, 2002, **149**, A346-A354.
11. S. K. Meher, P. Justin and G. Ranga Rao, *ACS Appl. Mater. Interfaces*, 2011, **3**, 2063-2073.
12. V. Ganesh, S. Pitchumani and V. Lakshminarayanan, *J. Power Sources*, 2006, **158**, 1523-1532.
13. J. Yan, Z. Fan, W. Sun, G. Ning, T. Wei, Q. Zhang, R. Zhang, L. Zhi and F. Wei, *Adv. Funct. Mater.*, 2012, **22**, 2632-2641.
14. J. H. Park, O. O. Park, K. H. Shin, C. S. Jin and J. H. Kim, *Electrochem. Solid-State Lett.*, 2002, **5**, H7-H10.
15. S. Nohara, T. Asahina, H. Wada, N. Furukawa, H. Inoue, N. Sugoh, H. Iwasaki and C. Iwakura, *J. Power Sources*, 2006, **157**, 605-609.
16. T. Brousse, D. Bélanger and D. Guay, in *Supercapacitors*, Wiley-VCH Verlag GmbH & Co. KGaA, 2013, pp. 257-288.
17. F. M. Gray, *Solid Polymer Electrolytes: Fundamentals and Technological Applications*, Wiley, 1991.
18. N. A. Choudhury, S. Sampath and A. K. Shukla, *Energy Environ. Sci.*, 2009, **2**, 55-67.
19. C.-C. Yang, S.-J. Lin and G.-M. Wu, *Mater. Chem. Phys.*, 2005, **92**, 251-255.
20. A. Lewandowski, K. Skorupska and J. Malinska, *Solid State Ionics*, 2000, **133**, 265-271.
21. C.-C. Yang, S.-T. Hsu and W.-C. Chien, *J. Power Sources*, 2005, **152**, 303-310.
22. C. C. Yang and S. J. Lin, *J. Appl. Electrochem.*, 2003, **33**, 777-784.
23. A. A. Mohamad and A. K. Arof, *Ionics*, 2006, **12**, 57-61.
24. L. S. Aladko, *Russ. J. Inorg. Chem.*, 2011, **56**, 2009-2012.
25. P. Vany´sek, in *CRC handbook of chemistry and physics*, ed. W. M. Haynes, CRC Press, 2013, pp. 77-79.
26. E. R. Nightingale, *J. Phys. Chem.*, 1959, **63**, 1381-1387.
27. G. Merle, M. Wessling and K. Nijmeijer, *Journal of Membrane Science*, 2011, **377**, 1-35.
28. R. J. Gilliam, J. W. Graydon, D. W. Kirk and S. J. Thorpe, *Int. J. Hydrogen Energy*, 2007, **32**, 359-364.
29. M. Wiebcke and J. Felsche, *Acta Crystallogr. Sect. C: Cryst. Struct. Commun.*, 2000, **56**, 1050-1052.
30. H. E. Swanson, R. K. Fuyat and G. M. Ugrinic, *Standard X-ray Diffraction Powder Patterns: Section 4. Data for 103 Substances*, US Department of Commerce, National Bureau of Standards, 1966.
31. M. Wiebcke and J. Felsche, *Acta Crystallogr. Sect. C: Cryst. Struct. Commun.*, 2000, **56**, 901-902.
32. W. M. Vogel, K. J. Routsis, V. J. Kehrer, D. A. Landsman and J. G. Tschinkel, *J. Chem. Eng. Data*, 1967, **12**, 465-472.
33. P. L. Taberna, P. Simon and J. F. Fauvarque *J. Electrochem. Soc.*, 2003, **150**, A292-A300.